ASME Turbo Expo 2023
Turbomachinery Technical Conference and Exposition
GT2023
June 26–30, 2023, Boston, Massachusetts

GT2023-101983

MULTI-DISCIPLINARY OPTIMIZATION OF THERMODYNAMIC CYCLES FOR LARGE-SCALE HEAT PUMPS WITH SIMULTANEOUS COMPONENT DESIGN

Jens Gollasch[1]*, Michael Lockan [1], Panagiotis Stathopoulos[1], Eberhard Nicke [1]

[1]German Aerospace Center (DLR), Institute of Low-Carbon Industrial Processes, Germany

ABSTRACT

The performance of high temperature heat pumps is highly dependent on the efficiency of its main components, which need to be optimally matched especially in closed cycles. The design process is therefore a challenging task as many disciplines and varying modeling depths need to be considered. Consequently, this is usually a sequential procedure beginning with cycle definition and raising the fidelity for component design. Fundamental design decisions are made based on assumptions for component performance. Mistakes in the phase of cycle definition are hard to be reversed in later design stages. Therefore, the present work introduces holistic approaches for multi-disciplinary design of closed Brayton cycles. Aerodynamic compressor design with 2D throughflow analysis and geometry based heat exchanger sizing are simultaneously optimized with thermodynamic cycle parameters. The presented methodologies are making use of highly sophisticated design tools drawing on many years of experience in gas turbine design. The results demonstrate that holistic heat pump optimization can be successfully performed with reasonable computational effort. The advantages compared to conventional sequential design are elaborated. Comparison of two optimization concepts indicates that splitting up the design vectors of cycle and components shows the tendency to improve robustness. Finally, the trade-off between system compactness and performance is demonstrated with a multi-objective optimization study.

Keywords: Optimization, Preliminary Design, Axial Compressor, Simultaneous Design, Cycle Performance

NOMENCLATURE

Roman letters

AAO	All-at-once optimization
$\boldsymbol{c}$	Constant parameter vector
COP	Coefficient of performance [-]
HEX, HE	Heat exchanger
$\boldsymbol{h}$	Constraint vector
HTHP	High temperature heat pump
l	length [m]
$\dot{m}$	Mass flow [kg/s]
MM	Metamodel
NHX	Nested heat exchanger design
P	Total pressure [Pa]
PC	Process chain
PCR	Pitch chord ratio
$\boldsymbol{p}$	Design vector
$\dot{Q}$	Heat flow rate [W]
R	Radius [m], heat capacity flow ratio [-]
SLC	Streamline curvature
$\boldsymbol{s}$	Station value vector
T	Temperature [K]
$\dot{W}$	Power [W]

Greek letters

α	Taper angle [°]
β	Outflow angle [°]
ε	Effectiveness [-]
η	Isentropic efficiency [-]
ω	Rotational speed [1/min]
Π	Pressure ratio [-]
$\boldsymbol{\zeta}$	Tolerance vector
ξ	Friction factor

Superscripts and subscripts

$*$	Optimized value
$\hat{}$	Target value
C	Compressor
ch	Chord
cyc	Cycle
H	High temperature heat exchanger (HTHX)
h	Hub
L	Low temperature heat exchanger (LTHX)
R	Recuperator
s	Shroud, shell
T	Turbine
t	tube, total

*Corresponding author: jens.gollasch@dlr.de

1 INTRODUCTION

High temperature heat pumps (HTHP) are a key technology in future energy systems. Their application ranges from electrifying district heating networks to supplying industrial processes with medium temperature heat [1] [2]. Large-scale heat pumps based on the reversed Brayton cycle will use axial turbomachinery similar to those in state-of-the-art gas turbines. The German Aerospace Center (DLR) can draw on many years of experience in this field. Highly sophisticated simulation and design methods for cycle and component analysis were established and can be used for HTHP. However, there is a high need for research and development in this area as the majority of current market-ready heat pump technologies operate only up to approximately 150 °C [3]. Reverse Brayton HTHPs are a promising technology especially for providing sensible heat with high temperature lifts. The gaseous working fluid can reach very low temperatures and for this reason the simultaneous integration of cooling processes is a possible application for this technology [4]. Also, concepts like fluid inventory control will invoke high part-load capability for integration into processes with high flexibility [5]. Adaption of cycle layout enables the combination with other systems like gas turbines [6]. For thermal capacities in the MW range components individually optimized for the application and its operating range will be required. Conventional design of HTHPs starts with the optimization of the thermodynamic cycle based on simple 0D modeling. Therefore, assumptions for the efficiency of the compressor or the effectiveness of the heat exchangers have to be made. The detailed design of the components follows, whereby their design conditions are set by the cycle. During this sequential procedure ambitious or pessimistic assumptions about the components can result in sub-optimal thermodynamic cycle design. As a result, this procedure cannot guarantee an optimal cycle configuration and component matching as it is based on trial and error. This paper presents the results of multi-disciplinary, holistic design approaches for reversed Brayton cycles, where the thermodynamic cycle parameters are simultaneously optimized with geometric design parameters of the components in a single step. DLR in-house software for thermodynamic cycle analysis (DLRp2), for 2D-throughflow compressor simulation (ACDC) and for heat exchanger rating based on the P-NTU method have been combined in two different process chains for comparison. In the first approach the thermodynamic as well as the component parameters are optimized all at once with a single design vector. A second concept with nested optimization loops for heat exchanger design is evaluated with regard to quality of results and computational effort. Single objective optimizations for cycle performance are performed to study the functionality of the optimization concepts with surrogate supported global optimization. So, a heat pump with approx. 7 MW thermal capacity and a temperature lift of 260 °C is designed as an exemplary use case.

The concept of coupled optimization for mostly single components together with the thermodynamic cycle has been studied e.g. for Organic Rankine cycles (ORC) or aero engine design. In the field of heat pumps, design studies for meanline radial compressor design in Rankine cycles can be found in the literature. Lampe et al. performed simultaneous optimizations of working fluid, cycle and turbine for ORC applications [7]. The design method has been complemented with a meanline design model of a radial-inflow turbine to bound the search space of the optimization problem to regions where the designs are feasible. The time needed to finalize the design process was significantly reduced as no trial and error is needed. Persky et al. also integrated turbine design for ORC cycles and underlined the importance of coupled optimizations in this field [8]. Schuster et al. investigated coupled design with consideration of off-design performance [9]. So, they were able to include guide vane positioning for the operating range. Bahamonde et al. integrated the design of small scale radial turbines in ORC applications for Diesel engines [10]. They divided the design process in two steps starting with design space exploration followed by the optimization. They found that the best cycle configuration is not necessarily the one with the highest turbine efficiency. In the field of aero engine design, Tacconi et al. performed simultaneous optimization for semi-closed cycles for high-altitude UAV propulsion [11]. Integrated component sizing has been coupled with a multi-objective optimization algorithm to minimize specific fuel consumption and weight. Schmeink et al. investigated different methods for component zooming to replace scaled compressor maps with an aerodynamic model based on streamline curvature [12]. Several coupling methods have been compared with regard to numerical effort and an exemplary multipoint design study has been performed. Hendler et al. performed optimizations with holistic aspects including the compressor and its connection to the combustor to achieve optimal performance [13]. The thermodynamic performance of the entire engine on system level was considered by using fixed interfaces. In the area of heat pump design Meroni et al. developed a meanline model for radial compressors [14]. They performed multi-objective optimizations to maximize cycle performance and heat flow rate for different cycles. Giuffre et al. used an approach for coupled design that replaces the aerodynamic compressor model with an artificial neural network (ANN) to speed up the design process [15]. This concept enables partial decoupling of the compressor design and reduces the amount of function evaluations to detect the pareto fronts.

1.1 Reversed Brayton cycle

Fig. 1 shows the cycle layout of a recuperated heat pump based on the reversed Brayton cycle. All studies presented in this paper relate to this use case and cycle architecture. The requirement of the heat sink is to lift the temperature of a 32 kg/s air flow from 100 °C to 320 °C. For the heat source an air flow of 35 kg/s at 60 °C is assumed. The reversed Brayton cycle works as follows: The compressor raises the temperature ($1 \rightarrow 2$) at the inlet of the high temperature heat exchanger (HTHX, $2 \rightarrow 3$). Remaining energy is used with a recuperator that transfers heat from the high pressure side to the compressor inlet. So, downstream of the HTHX the fluid is cooled down by the recuperator ($3 \rightarrow 4$) and then expanded in the turbine ($4 \rightarrow 5$). The cold fluid at the turbine outlet is heated up by the low temperature heat exchanger (LTHX) integrating the heat source ($5 \rightarrow 6$). To close the cycle, energy is transferred from the HTHX outflow, as described above ($6 \rightarrow 1$). Electric power to drive the heat pump process corresponds to the difference of the power to drive the compressor and the power recovered by the turbine. Turbine de-

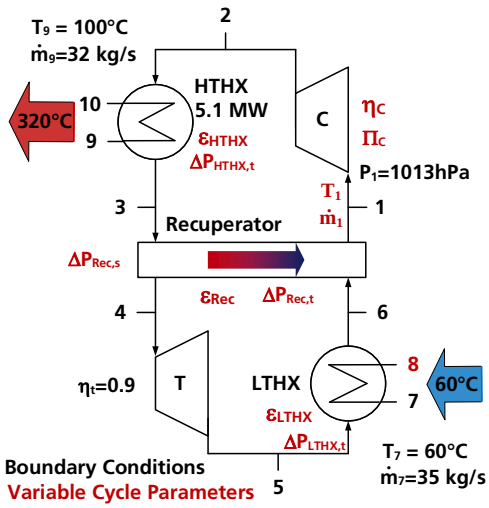

FIGURE 1: REVERSED BRAYTON CYCLE HEAT PUMP: LAYOUT WITH RECUPERATION

sign is not integrated and only the energy balance is relevant for the results. For this reason, there is no assumption made in this work wether compressor and turbine are mounted on the same shaft.

1.2 Outline and research questions

The present paper focuses on the investigation of holistic design approaches to simultaneously optimize cycle parameters and geometric component design. In a first step, methods for cycle and component analysis are introduced and the optimization problems are formulated. In the result sections, an exemplary sequential design study is performed demonstrating the benefits of direct integration of component design. Two different approaches for holistic optimization are studied and contrasted to sequential design. Additionally, a multi-objective optimization study showing the trade-off between cycle performance and compactness of its components is discussed. The following research questions are addressed:

- Which strategy can be used to optimally determine the thermodynamic cycle parameters with direct integration of aerodynamic compressor design and sizing of heat exchangers?
- In what aspects is a multi-disciplinary, holistic design methodology advantageous compared to sequential design of cycle and components?

2 HEAT PUMP DESIGN PROCESS

In order to perform holistic optimizations, detailed component analyses are integrated in process chains together with 0D-cycle models. Methods for modeling of thermodynamic cycle, axial compressors and shell and tube heat exchangers are introduced. Heat exchangers of this type are integrated because of the availability of the simulation tool. For applications of Brayton HTHP with gas-to-gas heat transfer alternative HE types would usually be used. First, an exemplary study for the conventional approach of HTHP design is presented for the introduced

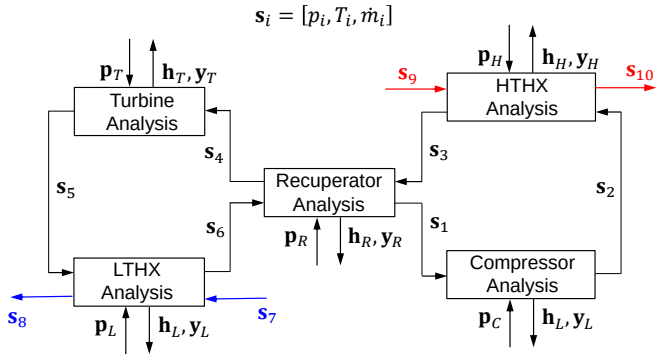

FIGURE 2: DATA STRUCTURE OF CYCLE AND COMPONENTS

use case. This procedure is then contrasted to strategies for the holistic, multi-disciplinary HTHP optimizations.

The generalized data structure of the optimization problems investigated in this work is visualized in Fig. 2. The cycle analysis solves the system for the station values $\boldsymbol{s}_1$ - $\boldsymbol{s}_6$ of the HTHP cycle. Each station consists of three parameters: $\dot{m}_i$, T_i and P_i. The inlet and outlet station values are at the same time design requirements for the cycles components. Each component has its individual design vector $\boldsymbol{p}_i$ and returns function values for constraints $\boldsymbol{h}_i$. The output values resulting from geometry based component design are named $\boldsymbol{y}_i$. In the following sections, different approaches for the design of thermodynamic cycles and its components are introduced.

2.1 Thermodynamic cycle optimization

The analysis of the thermodynamic cycle is performed with DLR in-house software. GTlab is a framework for the design of aero-engines [16] and is applied to heat pump analysis. Simulations are performed with its performance module GTlab-Performance and the code for thermodynamic cycle simulations (DLRp2) developed by Becker et. al [17]. The modeling approach for the reversed Brayton HTHP is based on setting the process requirements for the heat sink as well as the heat source as boundary conditions, which are fixed for the design process. Additionally, an equation system (EQS) consisting of variable process parameters (independents) and user-defined constant values (dependents) is set up. During the design calculations the EQS is solved iteratively with a Newton-Raphson method. Independents are varied to match the boundary conditions and dependents until convergence is reached. The model is parameterized to allow for access of key cycle parameters to serve as an interface to external processes like component analysis and optimization. The chosen approach enables process chains that start with compressor design runs, set the resulting parameters in the cycle model and compute heat exchanger design requirements as output of cycle analysis. In this way, inflow conditions ($s_1 = [T_1, p_1, \dot{m}_1]^T$) of the compressor and its pressure ratio and efficiency can be set as a result of the aerodynamic analysis with ACDC in the coupled process chains. Effectiveness of HTHX and recuperator are calculated to match the boundary conditions of heat sink and source. The LTHX effectiveness on the other hand is set directly. The optimization problem for cycle design is shown in Eq. 1 - Eq. 4:

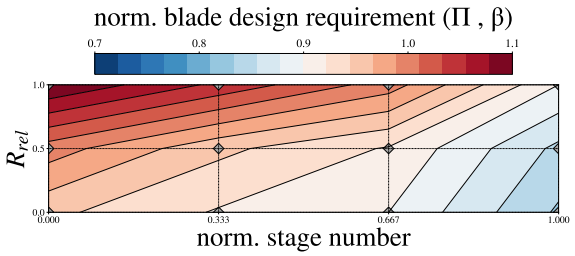

FIGURE 3: INTERPOLATION OF BLADE DESIGN REQUIREMENTS TO NORMALIZED COMPRESSOR TOPOLOGY

$$\max_{\boldsymbol{p}_{cyc}} COP \text{ with } COP = \frac{\dot{Q}_{HTHX}}{\dot{W}_C - \dot{W}_T} = \frac{\dot{m}_9 c_p (T_{10} - T_9)}{\dot{W}_C - \dot{W}_T} \quad (1)$$

$$\boldsymbol{p}_{cyc} = [\boldsymbol{s}_1, \varepsilon_L, \Delta \boldsymbol{P}_j] \in \mathbb{R}^9 \quad (2)$$

$$\boldsymbol{c}_{cyc} = [\eta_C, \eta_T, \boldsymbol{s}_7, \boldsymbol{s}_9, \boldsymbol{s}_{10}] \quad (3)$$

$$\text{s.t. } \boldsymbol{h}_{cyc} \leq \boldsymbol{\zeta}_{cyc} \quad (4)$$

$$\boldsymbol{h}_{cyc} = [\varepsilon_{max,j}] \quad (5)$$

$$\text{with } j \in \{\text{H, L, R}\}$$

The COP of the HTHP is applied as objective function. For the sequential approach the performance limit of the components is unknown and efficiency of the turbomachinery (η_C, η_T) and maximum effectiveness of the three heat exchangers as well as their pressure drop need to be assumed. Optimal pressure ratio, mass flow and compressor inlet temperature are determined as the results of this design approach. For all studies performed in this work, the turbine is parameterized via a constant efficiency of $\eta_T = 0.9$ and the outlet pressure.

2.2 Aerodynamic compressor design

The analysis and design of multistage axial compressors is performed with the DLR in-house software ACDC (Advanced Compressor Design Code). ACDC is an environment for preliminary design and throughflow analysis [18]. Its main components are an aerodynamic solver based on streamline curvature and a novel airfoil family called VCC. It consists of 2200 optimized airfoils for a 7-dimensional space of design requirements [19]. With this approach the design step of profile optimization is implicitly integrated. ACDC features a design mode making use of this database. An artificial neural network (ANN) has been trained with more than 10^6 blade profile simulations performed with MISES. In this way, correlations for profile loss and outflow angle are tuned for flow conditions and profile design requirements [20]. The ANN is integrated in the design mode of ACDC and optimized profiles are chosen based on inflow conditions and user specified design requirements. For rotors the pressure ratio is defined on specific relative heights. Internally the outflow angle is calculated. For stators on the other hand this outflow angle is set directly.

Fig. 3 shows the approach chosen in this work to set the blade design requirements . The normalized compressor topology with relative stage number and relative radial position R_{rel} is applied,

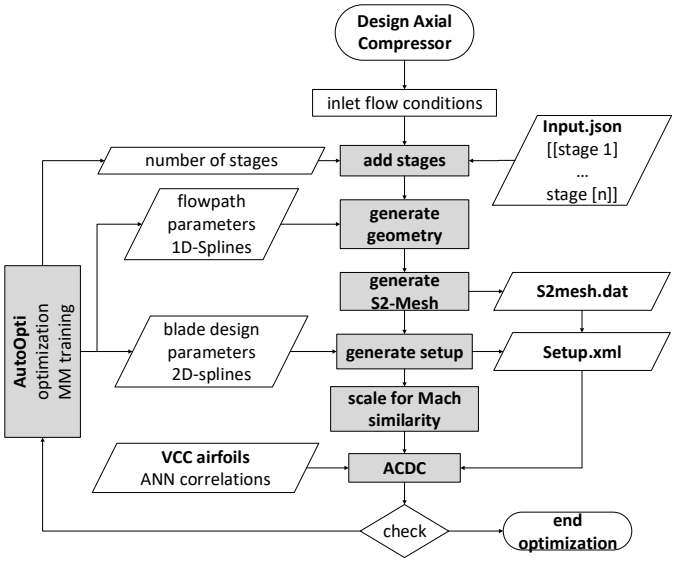

FIGURE 4: IN-HOUSE DEVELOPMENT OF COMPRESSOR OPTIMIZATION WITH GENERIC GENERATION OF GEOMETRY BASED ON EXISTING DESIGNS

which is independent from actual stage number. 2D-Spline interpolation for pressure ratio and outflow angle is calculated via 12 control points. These conditions are then mapped on each blade row at 4 radial positions to assign the optimal airfoil during the design run, as described above. This approach has been implemented to lower dimensionality for the optimization. Additionally the interpolation can be applied to any compressor configuration and will always consist of 24 parameters for rotors and stators, making this approach applicable for any design case.

Fig. 4 shows an automated process for generic generation of compressor geometry and numerical setup to perform design runs with ACDC. Its intention is to minimize user input for the initial geometry and to enable large search spaces in the context of integration into holistic optimization approaches. As a first step, a freely selectable number of meridional stage geometries is defined by the user. The multi-stage compressor geometry is then assembled. User defined input stages can be automatically reproduced for definition of additional downstream stages. Based on internal routines multi-stage compressors can be designed almost from scratch. It is also possible to vary the number of stages during runtime of the optimization, if needed. The geometric design requirements are set via 1D-splines to modify hub and shroud contours, chord length and inlet radii. A 2D mesh is computed and the numerical setup is generated with the 2D-interpolation, as described above. In the next step, the geometry can be automatically scaled for varying inflow conditions based on Mach similarity and reduced mass flow. This has been implemented to increase robustness during simultaneous optimization with varying inlet conditions. Finally, ACDC is executed in design mode. Fitting airfoils are allocated during convergence of SLC simulation. As a last step, relevant flow and performance parameters are evaluated via post-processing routines. The formulation of the optimization problem is defined with Eq. 6 - Eq. 9:

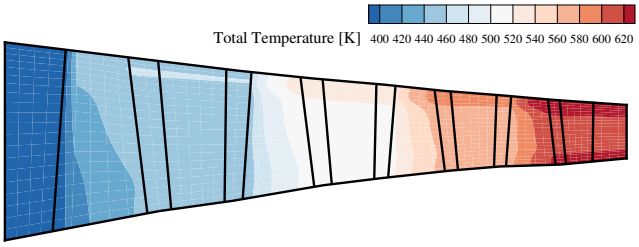

FIGURE 5: S2-VIEW OF A 4-STAGE COMPRESSOR GENERATED FROM SCRATCH DURING SIMULTANEOUS OPTIMIZATION

$$\max_{\boldsymbol{p}_C} \eta_C \text{ s.t. } \boldsymbol{h}_C \leq \boldsymbol{\zeta}_C, \tag{6}$$

$$\boldsymbol{p}_C = [\boldsymbol{\pi}_r, \boldsymbol{\beta}_s, \boldsymbol{n}_b, \boldsymbol{l}_{ch.}, \omega, \boldsymbol{r}_i, \boldsymbol{\alpha}_h] \in \mathbb{R}^{51} \tag{7}$$

$$\boldsymbol{c}_C = [\boldsymbol{\alpha}_s] \tag{8}$$

$$\boldsymbol{h}_C = [PCR, C_{\text{Koch}}, C_{\text{diff}}] \tag{9}$$

The data model of the compressor for the generic design procedure described above consists of 51 design parameters. The compressor is defined by setting the splines for blade design ($\boldsymbol{\pi}_{r,S}, \boldsymbol{\beta}_{s,S}$), number of blades $\boldsymbol{n}_{b,S}$, chord length $\boldsymbol{l}_{ch.,S}$, hub taper angle $\boldsymbol{\alpha}_{h,S}$, inlet radii $\boldsymbol{r}_i$ and rotational speed ω. To guarantee feasibility of the design, a vector of constraint functions for stability and geometric bounds is used for the optimizations as shown in Eq. 9. Hereby, the design process is restricted to meet a specified range of pitch chord ratios PCR and diffusion factors $C_{diff.}$, that relate to the design space of the pre-optimized VCC airfoil family. Additionally the stability of the compressor is considered by use of the Koch-criterion C_{Koch} as described in [21].

Fig. 5 shows the meridional view of an optimized compressor topology as it is generated in the multi-disciplinary optimizations that are the focus of this paper. Two stages are given as user-defined input for the initial geometry and the compressor is designed from scratch with the methodology described before. Leading and trailing edges of rotor and stator blades are emphasized with the vertical lines. In the HTHP cycle this compressor delivers a pressure ratio of $\Pi \approx 4.8$ and a temperature lift of $\Delta T \approx 220K$, which is highlighted with the contour variable T_t.

2.3. Heat exchanger design

The heat exchanger analysis used in this work is based on the $P - NTU$ method for shell and tube heat exchangers [22]. P is the non-dimensional temperature change and NTU describes the number of transfer units for both sides of the heat exchanger. Based on geometric parameterization the heat transfer as well as pressure drop of shell and tube heat exchangers can be modeled. Eq. 11 - Eq. 12 shows the basic procedure to calculate the heat flow rate of the heat exchangers based on geometric parameters $\boldsymbol{p}_{HE}$ of the HE design vector.

$$NTU_i = kA/(\dot{m}_i\, c_{p,i}) = f(\boldsymbol{p}_{HE}) \tag{10}$$

$$T_{out,i} = f(P_i) = f(NTU_i, R_i) \text{ with } i = [\text{tube, shell}] \tag{11}$$

$$\dot{Q} = \dot{m}_i\, c_{p,i}\, (T_{\text{out,i}} - T_{\text{in,i}}) \tag{12}$$

The outlet temperatures of shell and tube side are computed via the dimensionless temperature change P_i which depends on the NTU_i values and the heat capacity flow ratio R_i. NTU is calculated with the use of heat transfer coefficient as a function of the Nusselt number. The heat flow rate can then be calculated with the heat capacity flow and the temperature spread from inlet to outlet ($\Delta T = T_{\text{out,i}} - T_{\text{in,i}}$).

$$\Delta P_t = \frac{l_t \rho u^2}{d_{2t,i}} \xi_t \text{ with } \xi_t = \frac{0.1364}{\sqrt[4]{Re_t}} \tag{13}$$

Eq. 13 shows the calculation of tube side pressure drop. Tube friction is estimated based on friction factor ξ_t and Reynolds number.

$$\Delta P_s = (n_{\text{baffles}} - 1)\Delta P_{\text{cross}} + n_{\text{baffles}}\, \Delta P_{\text{wind.}} + \Delta P_{\text{nozzle}} \tag{14}$$

Eq. 14 shows the breakdown of the shell side losses taken into account in this work. ΔP_{cross} is the pressure drop in a cross flow area between two baffles, $\Delta P_{\text{wind.}}$ in the baffle window zones and finally ΔP_{nozzle} in the in- and outflow nozzles.

The described analysis is also integrated in a standalone design environment, which optimizes the geometry of the heat exchanger to meet requirements for heat flow rate $\dot{Q}$ and pressure drop on both sides. Component design for heat exchangers is described in Eq. 15, Eq. 17 and Eq. 18:

$$\min_{\boldsymbol{p}_j} l_t \text{ s.t. } \Delta \boldsymbol{s}_j \leq \boldsymbol{\zeta}_j \tag{15}$$

$$\boldsymbol{p}_j = [d_t, l_t, n_t, s_t, n_{baffles}] \tag{16}$$

$$\Delta \boldsymbol{s}_j = [(\hat{\dot{Q}}_j^* - \dot{Q}_j)^2, (\Delta \hat{P}_j^* - \Delta P_j)^2] \tag{17}$$

$$[\dot{Q}_j, \Delta P_j] = \boldsymbol{f}_j(\boldsymbol{p}_j, \hat{\boldsymbol{s}}_{i,in}^*) \tag{18}$$

$$\text{with } j \in \{\text{H, L, R}\}$$

The tube length is minimized as the objective function for a given tolerance $\boldsymbol{\zeta}$ of deviation from design requirements. The latter is a vector of target values to ensure that heat flow rate $\hat{\dot{Q}}_{HE}^*$ and pressure drop $\Delta \hat{P}_{HE}^*$ for shell and tube side are met. The HE optimization is performed with differential evolution [23] followed by a local algorithm to polish the result. The design vector consists of the five most sensitive parameters for heat flow rate and pressure drop. According to this, tube inner diameter d_t, tube length l_t, number of tubes n_t, tube separation s_t and number of baffles $n_{baffles}$ are varied to meet the requirements.

2.4. Conventional heat pump design

To underline the motivation for the work presented in this paper, the conventional design procedure is applied to the HTHP case as a first step. Cycle performance is optimized based on

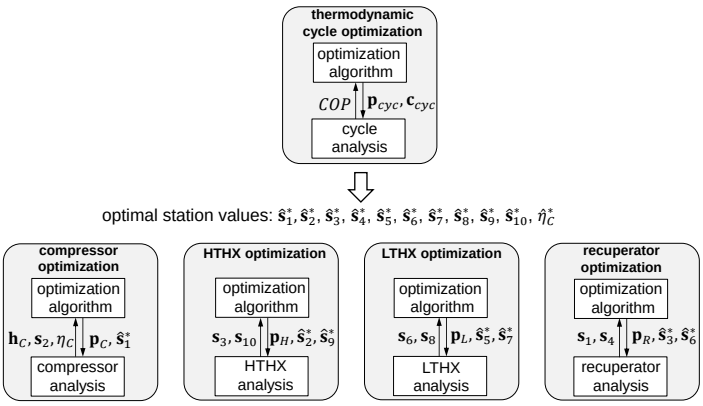

FIGURE 6: SEQUENTIAL DESIGN OF CYCLE AND COMPONENTS

assumptions for component performance as introduced with the cycle design methodology. The optimized results values are the design requirements for the components. Their feasibility and actual performance is checked with subsequent optimization of compressor and heat exchangers. Eq. 19 shows the formulation of the cycle optimization for the sequential design procedure:

$$\max_{\boldsymbol{p}_{cyc}} COP \text{ s.t. } \boldsymbol{h}_{cyc} \leq \boldsymbol{\zeta}_{cyc} \tag{19}$$

$$\boldsymbol{p}_{cyc} = [\hat{\eta}_C, \Pi_C, \hat{\boldsymbol{s}}_1, \varepsilon_L, \Delta \boldsymbol{P}_j] \in \mathbb{R}^{10} \tag{20}$$

$$\boldsymbol{c}_{cyc} = [\hat{\eta}_T, \hat{\boldsymbol{s}}_7, \hat{\boldsymbol{s}}_9, \hat{\boldsymbol{s}}_{10}] \in \mathbb{R}^{10} \tag{21}$$

$$[\hat{\boldsymbol{s}}_2, \hat{\boldsymbol{s}}_3, \hat{\boldsymbol{s}}_4, \hat{\boldsymbol{s}}_5, \hat{\boldsymbol{s}}_6] = \boldsymbol{f}_{cyc}(\boldsymbol{p}_{cyc}, \boldsymbol{c}_{cyc}) \tag{22}$$

$$j \in \{\text{H, L, R}\}$$

The COP is maximized as the objective function and depends on the variable design parameters (Eq. 20) and constant boundary conditions (Eq. 21) of the cycle. The results of cycle analysis are used as inputs for component design.

The process of sequential component design is visualized in Fig. 6. As a result of the cycle optimization, the optimal stations values s_i^* are determined, which are the optimized target values $\hat{s}_i^*$ for the now following design of compressor and heat exchangers. The inflow conditions defining the design points vary with different assumptions. The component design is either successful or unfeasible for these requirements, which leads to a process of trial and error. Following cycle optimization, the compressor design has to be performed to match the target values for the sequential approach:

$$\min_{\boldsymbol{p}_C} \Delta s_C \text{ s.t. } \boldsymbol{h}_C \leq \boldsymbol{\zeta}_C \tag{23}$$

$$\text{with } \Delta s_C = (\hat{\Pi}_C^* - \Pi_C)^2 + (\hat{\eta}_C^* - \eta_C)^2 \tag{24}$$

$$[\boldsymbol{h}_C, \eta_C, \Pi_C] = \boldsymbol{f}_C(\boldsymbol{p}_c, \hat{\boldsymbol{s}}_1^*) \tag{25}$$

Feasible configurations for a target pressure ratio $\hat{\Pi}_C^*$ and a target efficiency $\hat{\eta}_C^*$ with the given inflow conditions of $\hat{s}_1^*$ need to be found to consider the compressor design successful. Finally, heat exchanger design is performed with the standalone optimization approach described above. Target values of heat flow rate and pressure drop are met up to a certain tolerance for deviation from design requirements.

TABLE 1: SEQUENTIAL DESIGN STUDY - FEASIBILITY CHECK OF ASSUMED COMPONENT PERFORMANCE

Assumption	Default	Feasible	Ambitious	Feasible
η_c	0.85	✓	0.87	✓
ε_{HTHX}	0.9	✓	0.95	×
ε_{Rec}	0.85	✓	0.95	×
ε_{LTHX}	0.92	✓	0.95	✓
COP	1.65	✓	1.74	×

An exemplary design study with sequential component design is performed with the methodology introduced above. Component performance for compressor and heat exchangers has first to be assumed on cycle level and experience values are used. For reasons of simplicity, the pressure drop of each HE has been set to constant values of 1 % on high pressure side and 2 % on low pressure side of each HE for this study. As a first step, the process parameters are optimized on cycle level as described in Eq. 19 - Eq. 22. The optimal cycle values are then used to define the design points for the components.

The results of the conventional HTHP design are shown in Tab. 1. Initially, moderate assumptions (default design) for component efficiency are made and, as expected, feasible designs can be found. However, it is clear that an optimal COP will not be reached with these values as component performance is not maxed out. Consequently, the cycle is then optimized with more ambitious assumptions in a next step, which results in a significantly higher COP. Now the design requirements on component level are harder to meet and within the HEX search space no feasible geometry resulting from these assumptions can be found. This applies for the recuperator ($\Delta\dot{Q} = 43\,\text{kW} > 10\,\text{kW}$) and the HTHX ($\Delta\dot{Q} = 208\,\text{kW} > 10\,\text{kW}$). The assumed effectiveness of $\varepsilon = 0.95$ is only feasible for LTHX design as the mass flows of both sides are significantly different in magnitude, which means that the effectiveness reaches higher values. The optimal COP should lie somewhere in between the default and ambitious assumptions. To find the optimal configuration for the heat pump each component needs to perform at its maximum efficiency while being optimally matched on system level. It is not guaranteed to reach the global optimum with the described trial and error procedure, especially if additional aspects like engine compactness or costs need to be considered.

3 SIMULTANEOUS HEAT PUMP OPTIMIZATION CONCEPTS

Cycle and component optimizations are challenging tasks. To avoid the trial and error process of sequential cycle and component design, the optimization is performed in a single step by integration of component analysis in coupled process chains. This means that uncertainties originating from inaccurate assumptions during the phase of cycle definition are avoided and thereby potential error sources are eliminated. Accordingly, the design space is opened up and information on component sizing and efficiency is available to be considered in the process of finding the best sys-

tem level design point. As a downside, the computational effort is increased for the multi-disciplinary approach. The initial idea of the process chains implemented for this work is to start with the aerodynamic design of the compressor and evaluate its performance with cycle analysis. Consequently, every compressor design set by the optimizer is evaluated on cycle level by writing the output parameters to the cycle model. In this way, the inlet conditions ($\dot{m}_1, T_1, P_1$) as well as efficiency and pressure ratio can be set according to the results of aerodynamic compressor design. As a last step, the optimal heat exchangers for HTHX, LTHX and recuperator need to be found. For this, two different approaches are introduced. In a first method, the entire search space of component and cycle design is handled with a single optimization process and is thereby called all-at-once (AAO) approach. The second process chain decouples the heat exchanger design vector from the master optimization. Feasibility of HE design is checked for the specific requirements derived from the results of cycle evaluation. This is achieved with inner optimization loops and is here called nested heat exchanger design (NHX). For these multi-disciplinary approaches only a single assumption has to be made on thermodynamic cycle level: The isentropic efficiency of the turbine as its aerodynamic design is not integrated yet.

3.1 Metamodel assisted global optimization

The holistic optimizations investigated in this work require for efficient optimization methods. The latter are performed with the DLR in-house suite AutoOpti, which features genetic algorithms for global optimization supported with metamodels, which have proven to speed up the process [24]. Each optimization starts with creating an initial database of converged solutions with a latin hypercube approach. From this point on, half of the individuals of the following generations are created with genetic operators and methods like differential evolution while the other half is generated by optimization on the metamodels. For this, Kriging response surfaces for each variable of the objective and constraint functions are created in a separate process. New individuals with high expected improvement are evaluated according to the metamodels predictions and stored in the database to continuously improve the accuracy of Kriging regression. The usability of surrogates to work with the coupled design process chains is an additional challenge, that is discussed in the following sections.

3.2 All-at-once optimization concept

As a first approach for simultaneous design, the all-at-once optimization (AAO) is introduced. The basic concept for this is to use a single optimization process and thereby a single design vector in a process chain, which executes compressor analysis, cycle performance and HE rating.

The process chain is shown in Fig. 7. The workflow of AAO starts with the compressor analysis with its design vector $\boldsymbol{p}_C$ and inlet condition $\boldsymbol{s}_1$. The output parameters characterize the performance of the current compressor design which is used as input in the following cycle analysis. On this level the COP and HE performance are then computed. The heat exchanger analysis is performed as the last step returning the actual heat flow rate and pressure drop as a result of the geometric design parameters. The formulation of the AAO optimization is defined as follows:

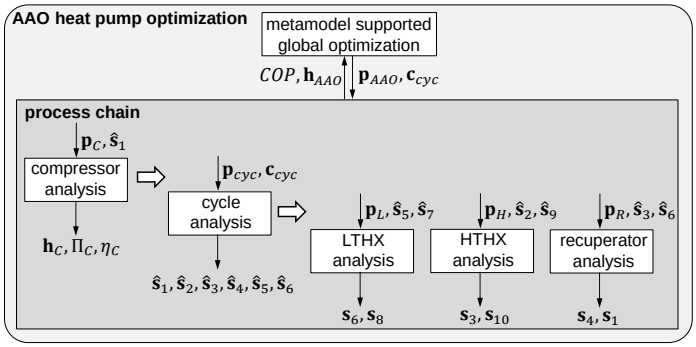

FIGURE 7: ALL-AT-ONCE (AAO) OPTIMIZATION PROCESS CHAIN

$$\max_{\boldsymbol{p}_{AAO}} COP \text{ s.t. } \boldsymbol{h}_{AAO} \leq \boldsymbol{\zeta}_{AAO}, \tag{26}$$

$$\boldsymbol{p}_{AAO} = [\boldsymbol{p}_C, \boldsymbol{p}_{cyc}^{AAO}, \boldsymbol{p}_j] \in \mathbb{R}^{76} \tag{27}$$

$$\boldsymbol{p}_{cyc}^{AAO} = [\hat{\boldsymbol{s}}_1, \varepsilon_L, \Delta \boldsymbol{P}_j] \tag{28}$$

$$\boldsymbol{h}_{AAO} = [\boldsymbol{h}_C, \Delta \boldsymbol{s}_j - \boldsymbol{\zeta}_j] \tag{29}$$

$$\text{with } j \in \{\text{H, L, R}\}$$

Cycle performance (COP) is the objective function and the design vector $\boldsymbol{p}_{AAO}$ contains 76 variables from each discipline. The main challenge for this strategy is to find consistent designs, which meet all constraints. The heat exchangers are designed to match the heat flow rates $\dot{Q}_i$ and pressure drops, as they are calculated in cycle performance. This is achieved by minimizing the deviation of these target values to a defined threshold of 10 kW for heat flow and 100 Pa for pressure drop. This is considered via constraints and the expression $\Delta s_{j,i} - \zeta_{j,i} \leq 0$ for each HE. If this condition is met and the compressor specific constraints are also assured, the process chain is feasible. It is expected, that this approach will need a lot of iterations to converge. There are two reasons for that: First, fitting heat exchanger designs need to be found and secondly the sensitivity and interaction of each design parameter needs to be detected to improve the objective while constraints are kept below the thresholds.

3.3 Nested heat exchanger optimization concept

A second approach with decoupled optimization of the heat exchangers is investigated. This process chain is shown in Fig. 8 and is here called nested-HE-design (NHX). The first two steps of aerodynamic compressor design and cycle analysis are identical to the AAO process. For the last step of HE-design, the three heat exchangers are optimized in nested optimization loops for requirements that result from cycle evaluation. Hence, the process chain is consistent if the nested optimizations converge and the design requirements for the heat exchangers can be met. This approach reduces the amount of design variables in the master optimization process by splitting up the design vector. Optimal heat exchanger designs are determined with regard to the local objective function, which is in this case the tube length. The formulation of the NHX optimization is shown in Eq. 30 - Eq. 33:

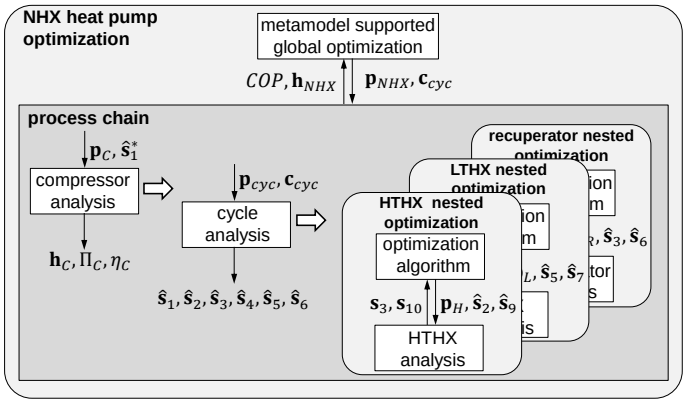

FIGURE 8: NESTED HEAT EXCHANGER DESIGN (NHX) PROCESS CHAIN

$$\max_{\boldsymbol{p}_{NHX}} COP \text{ s.t. } \boldsymbol{h}_{NHX} \leq \boldsymbol{\zeta}_{NHX}, \tag{30}$$

$$\boldsymbol{p}_{NHX} = [\boldsymbol{p}_C, \boldsymbol{p}_{cyc}^{NHX}] \in \mathbb{R}^{61} \tag{31}$$

$$\boldsymbol{p}_{cyc}^{NHX} = [\hat{s}_1, \varepsilon_L, \Delta \boldsymbol{P}_j] \tag{32}$$

$$\boldsymbol{h}_{NHX} = [\boldsymbol{h}_C, \Delta \boldsymbol{s}_j^* - \boldsymbol{\zeta}_j] \tag{33}$$

The design vector only consists of design variables for the compressor and thermodynamic cycle. The heat exchangers are designed as introduced in Eq. 15 - Eq. 18. The deviation from the design requirements is returned to the master optimization process, which is performed with metamodel assistance. This is considered via the expression $\Delta \boldsymbol{s}_i^* - \boldsymbol{\zeta}_i \leq 0$, which assures that the deviation of the optimized geometry $\Delta \boldsymbol{s}_i^*$ is smaller than the threshold $\boldsymbol{\zeta}_i$. This is important for the use of Kriging metamodels in this work, so that the optimization process is able to track unfeasible designs.

4 SIMULTANEOUS HEAT PUMP DESIGN STUDY

To investigate the holistic design methodologies as introduced in the prior sections, exemplary studies are performed for the use case of the reversed Brayton HTHP. Heat sink and heat source requirements are kept constant throughout the design processes. The two process chains with simultaneous optimizations are applied and their performance is compared to each other. The overall goal is to evaluate the approaches concerning their functionality, robustness and computational effort. To further demonstrate a possible application of holistic optimization, a multi-objective design study highlighting the trade-off between compactness and engine performance is discussed.

4.1 Comparison of optimization concepts

Fig. 9 shows the convergence of the objective function COP with the all-at-once concept. The grey line represents the first attempt that starts with 600 randomly created configurations. Only a fraction of these configurations converge to form the initial database. As can be seen, convergence is not achieved even after a high number of evaluations. This can be explained by the characteristic of this approach that it is hard to find consistent heat

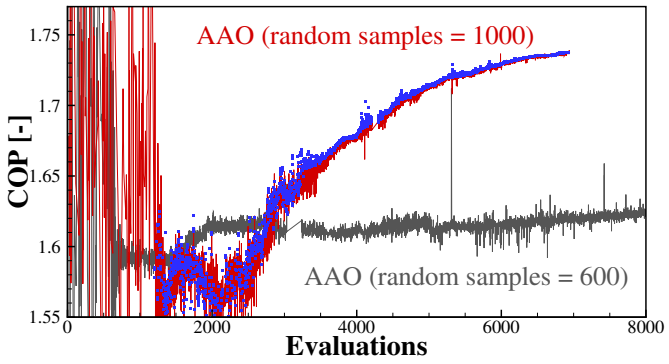

FIGURE 9: CONVERGENCE OF ALL-AT-ONCE OPTIMIZATION

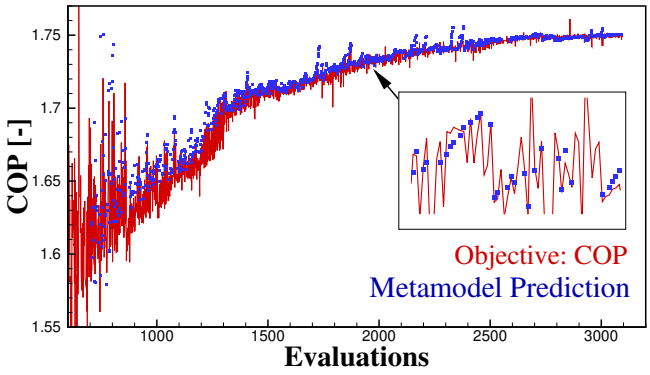

FIGURE 10: CONVERGENCE OF NESTED HE-DESIGN GLOBAL OPTIMIZATION WITH KRIGING METAMODELS

exchanger designs within the single design vector. In this case, during the first 6000 evaluations the constraints to match the HEs to the cycle requirements are minimized which slows down the actual optimization and no convergence is reached. Thus, the initial database is enlarged to 1000 configurations for a second attempt. For this case, consistent heat exchangers can be found earlier and the optimization converges as indicated by the red line. Also, the metamodels (MM) are functional, which can be seen by the blue squares representing the MM predictions. With the growing database it gets very time consuming to update the Kriging models, which could be a reason why the MM accuracy shows a periodic deviation from the simulated results.

Fig. 10 shows the convergence of the cycle performance for the nested HE-design (NHX). After a randomly created initial database of 500 configurations based on a latin hypercube, more than 2500 process chains need to be evaluated until convergence is reached. The red line shows the COP of each evaluated process chain. As expected there are high fluctuations in the first third of the optimization process, where the constraints for compressor design and heat exchanger feasibility are controlled. Also, in this area the predictions made by the metamodels are significantly improving with the growing database. The functionality of metamodel usage is underlined in the zoomed subplot. After roughly 1000 evaluated configurations the surrogates perform really well. This is shown by the blue squares, which are almost spot on. The

TABLE 2: COMPARISON OF THE OPTIMIZATION APPROACHES

	Success	Eval.	COP	time PC [s]	time MM [s]
AAO	✓	6934	1.738	271718	150746
NHX	✓	3096	1.751	673885	24468

NHX approach shows robust convergence and can be computed during a time span of approx. 18h on up to 36 CPUs.

Tab. 2 shows the comparison of the AAO and the NHX optimization approach. Both approaches reach convergence with the applied criterion, which is reached when the best 15 individuals in the database show a very small deviation concerning the objective function value:

$$COP[15] \leq COP[1] + 1e{-}4 \tag{34}$$

As expected, the AAO strategy needs a very high number of evaluated process chains to find an optimum. By decoupling the HE design, this number is more than halved to 2496 converged runs after creating the initial database. Another important outcome is, that AAO converges into a worse value for the objective function compared to NHX. The design space for the recuperator and the LTHX has not been entirely used as convergence was found with HE designs below the maximum allowed tube length, which is the most sensitive parameter for transferred heat. A better COP is achieved with the NHX approach due to improved HE designs, which also effect overall cycle parameters and compressor design point. Another important aspect is the computational effort. NHX converges with less process chain evaluations but each of these has a higher CPU time because of the nested optimization loops of the three heat exchangers. Each chain computation takes up to seven minutes with the HE design running in parallel on three processors. AAO evaluation on the other hand is very fast, as only a single design is computed for each HE and the consistency with cycle requirements is handled with global constraint functions. HE rating is done in fractions of a second, but the AAO chains need to be run for a high number of times. Additionally, the generation of the Kriging models and the optimization on these response surfaces to find new individuals needs to be considered here. This brings the problem that metamodel based optimization becomes very time consuming and updates of the response surface get more costly with a growing database. The first aspect can also be read from Tab. 2 as the effort to optimize on the MMs is many times larger for AAO compared to NHX.

Therefore, it can be stated, that the NHX approach is more suitable for the chosen problem of HTHP design in combination with the integrated methods for component analysis. This can be specifically concluded for the main objective of the studies, which is robustness. Consequently, the NHX optimization results are further discussed and analyzed in detail.

4.2 Component design with NHX

Fig. 11 shows the convergence of component efficiency for the NHX optimization. The black line represents the optimization of the compressor design. Its inflow conditions $\boldsymbol{s}_1$ are simul-

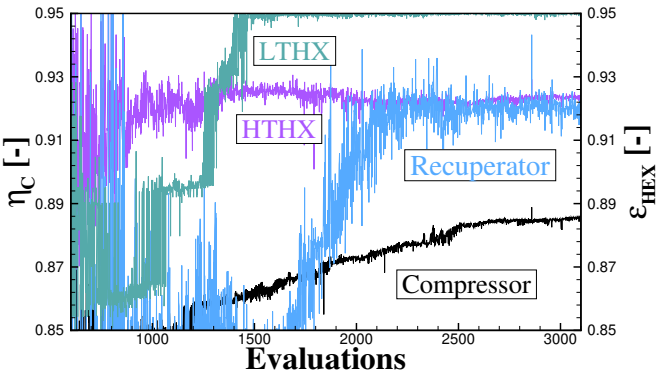

FIGURE 11: COMPONENT PERFORMANCE WITH INTEGRATED DESIGN

taneously optimized with cycle evaluation while efficiency and pressure ratio are returned to system level. Because of the high number of design variables, the compressor optimization needs a high amount of converged solutions until its maximum efficiency of $\eta_C \approx 88.3\,\%$ is reached and all constraints are fulfilled. The 4-stage axial compressor is thereby designed for an optimal pressure ratio of $\Pi \approx 4.6$. So, the high efficiency is the consequence of medium blade loading. Compared to this, HTHX and LTHX run relatively fast into their maximum effectiveness within the given parameter space. The HTHX achieves a maximum effectiveness of $\varepsilon_{HTHX} \approx 0.92$. The inlet temperature on HTHP side T_2 is set in a way, that together with the resulting mass flow $\dot{m}_1$ approximately equal heat capacity flows on both entries appear. This is an expected result, as the temperature difference over the full length of the HE is minimized in this way and parallel temperature profiles do occur. The latter is known to be the configuration with best exergetic efficiency for heat pump design with sensible heat transfer. This goes in line with the recuperator running into a similar effectiveness, which can be explained with identical mass flows on both sides which invoke similar design requirements. A highly efficient recuperator is important to transfer heat from the HTHX outlet to the compressor inlet, which can be designed for lower pressure ratios in turn. The LTHX effectiveness is higher, which can be explained by the fact, that the heat capacity flow ratio is significantly unequal which causes higher values. So, the LTHX achieves an effectiveness of $\varepsilon_{LTHX} = 0.95$, which is in this case restricted by the upper bound of the cycle variable that sets this design requirement. Consequently, higher maximum LTHX effectiveness could be applied to further improve heat source integration within the geometrical design space. To sum up these results, it can be stated that component optimizations run into the expected high values which underlines the functionality of this optimization approach.

Fig. 12 shows the resulting normalized tube length for all three shell and tube heat exchangers. As can bee seen, all heat exchangers make use of their search space and converge into the maximum tube length. This also supports the feasibility of the results, as highly efficient HEs will significantly improve the COP. HTHX design determines the effective integration of the heat sink and is thereby very sensitive, which explains why this HE

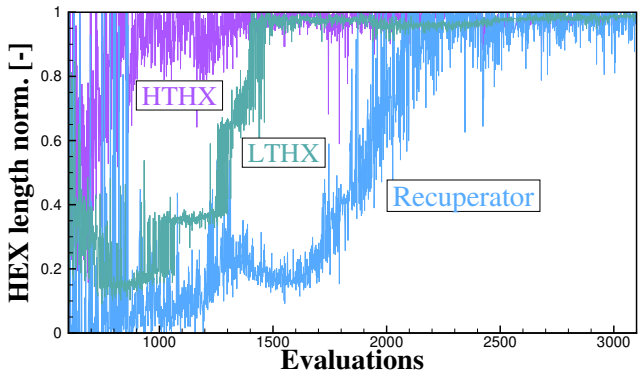

FIGURE 12: HEX NORMALIZED TUBE LENGTH

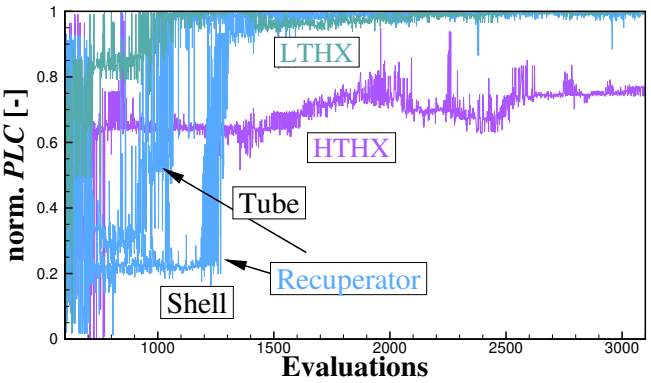

FIGURE 13: HEX PRESSURE LOSS COEFFICIENT

runs into its most effective design relatively early during the optimization. The recuperator takes more iterations to finally reach the upper bound after 2000 converged process chains. As can be seen, only the LTHX seems to not fully run into the upper bound, which is explained by the limitation of maximum effectiveness, which is directly set as design requirement. As explained before, this value could have been chosen slightly higher. However, the nested LTHX design gets very close to the upper bound. So, there is not much room for further improvement and the HTHP should be designed close to its maximum performance.

Fig. 13 shows the convergence of the pressure drop coefficients $PLC = \frac{P_{out}}{P_{in}}$, which are on the one hands side design parameters of the thermodynamic cycle model and at the same time design requirements to be met by HEX design. Consequently, low pressure drop has a positive effect on the COP as the turbine is able to recover more energy when operated with high pressure ratios. Additionally, the pressure drop value has to met by the HE design while the required heat flow is delivered. In the NHX approach, the values of $\dot{Q}$ and PLC have to be reached below threshold values, as described above. For HTHX and LTHX only the tube side value is a cycle variable, while shell side pressure drop on secondary side is set to a fixed value to lower complexity. Secondary sides of these heat exchangers do not have an effect on the COP. For the recuperator both PLC variables for shell and tube side are considered as they appear in the HTHP cycle.

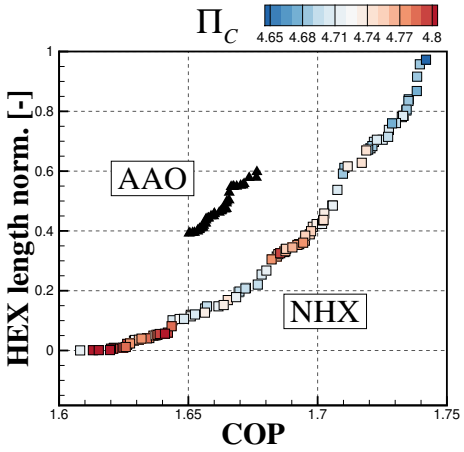

FIGURE 14: PARETO OPTIMAL HTHP DESIGNS FOR THE TRADE-OFF BETWEEN COP VS. MAXIMUM HEX LENGTH

The convergence of the normalized PLC variables shows that values for LTHX and recuperator near the upper bound of the cycle variable are reached. This means, that feasible HE designs have been found to work with the lowest requested pressure drop. For these two heat exchangers the upper bound could have been set higher for further improvement of the cycle performance. The pressure drop of the HTHX tube side converges to a value within its parameter bounds. In summary, it can be deduced that the trends of convergence to low pressure drop also underlines the functionality of the NHX optimization approach.

To sum up the investigations of the two introduced holistic strategies, it can be concluded that multi-disciplinary design with simultaneous optimization of cycle and components can be successfully performed for the HTHP use case. Especially with regard to robustness the NHX optimization is more suitable compared to AAO. Kriging metamodels are able to predict the functional output, which has a positive impact on speed of convergence. Functionality of the NHX process chain can be demonstrated with the analysis of resulting component performances, which run into high values while making full use of the defined search space. The trend of splitting design vectors to increase robustness will be part of future work.

4.3 Multi-objective optimization study

Integrating component design with cycle optimization does not only lower uncertainties and improves the determination of ideal design points. Additionally, information on preliminary component geometries is available. This means, that system compactness or detailed cost functions can be considered with higher accuracy than conventional approaches that are usually only able to roughly estimate these values.

Fig. 14 shows the results of a multi-objective optimization study with AAO and NHX approach. Additionally to the cycle performance COP as an objective function, the trade-off with compactness of the engine is considered here. As an indicator for this, the maximum tube length of all heat exchangers is minimized as the additional objective. More compact heat exchanger designs naturally perform worse with regard to transferable heat

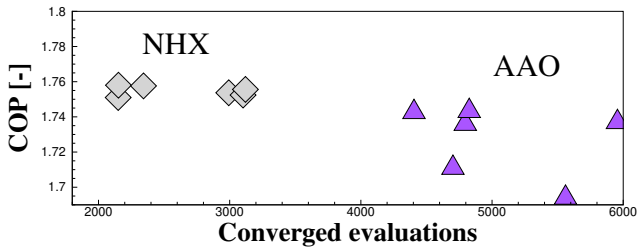

FIGURE 15: REPRODUCIBILITY OF THE RESULTS

and pressure drop. The plot shows the Pareto fronts of AAO and NHX approach. It becomes clear, that AAO only detects a fraction of optimal configurations and performs worse compared to the results computed with NHX. The latter method clearly shows the trade off between HEX length and COP over the entire considered range. The cycle performance ranges from $COP_{min} \approx 1.6$ for the most compact engine and $COP_{max} \approx 1.75$ for the largest heat exchangers. These results are in line with the single objective optimizations discussed before and emphasize the functionality of the NHX optimization. AAO is not suitable here and even after a large number of converged process chains the results are significantly worse compared to NHX. The scattered points of the NHX front also show the pressure ratio of the compressor as a contour variable. With more compact heat exchanger designs the tendency for higher pressure ratios is noticeable as HEs perform worse and pressure drop increases. This has an additional effect on compressor performance, which decreases with higher blade loading. Deviations from this trend with visible peaks could be explained with the fact that full convergence is not reached.

The multi-objective optimization demonstrates a further benefit of holistic design approaches. With this approach, the available building space for industrial heat pumps can be considered directly in earliest design phases. Basic decisions for cycle performance in interaction with engine sizing or component costs can be made with better accuracy.

4.4 Discussion and outlook

In the prior sections results are presented, that demonstrate the functionality of holistic optimization for the specific case of a reversed Brayton cycle HTHP with recuperated cycle layout. The results can be interpreted as a proof of concept for the used tool set and optimization approaches. It is shown, that the architecture of the process chain has a large effect on convergence and computational effort. Fig. 15 shows the reproducibility of the single objective optimization studies. Both approaches have been repeated five additional times and objective function value as well as number of converged evaluations are analyzed. As expected, the NHX optimization converges into similar optimal configurations with the chosen convergence criterion, which could be the reason for minor deviations. AAO shows a large spread and a high number of evaluations is necessary, which leads to enormous computational effort when the response surfaces are recomputed. Some of the AAO attempts did not reach convergence within a reasonable runtime.

The current work focuses on stable integration of detailed 2D compressor design together with fast HE analysis and cycle simulation but does not represent a generic approach for a wider range of applications and methods. Splitting the design vector by decoupling the heat exchanger design improves convergence, which is why similar approaches could be chosen for turbomachine design. Component analysis considered in future process chains can get more costly and the optimization task becomes even more challenging for the growing design spaces. As a first step, the integrated methods for HE design will be replaced for more in-depth analysis of different types of heat exchangers that are more suitable for gas-to-gas heat transfer. For these reasons, additional research needs to be performed to investigate efficient ways to perform holistic optimizations. Component design can potentially be decoupled with the use of intermediate metamodels integrated in the optimization architectures. These metamodels can be beneficial to reduce the number of times the actual aerodynamic or heat transfer analyses need to be performed. For the reasons discussed above it can be derived, that there is a large potential for future research in the field of holistic heat pump design. Speeding up convergence would also enable to integrate higher dimensional methods for heat exchanger or turbomachine analysis.

5 CONCLUSIONS

The present work demonstrates, that the introduced holistic optimization concepts are functional for the design of HTHP based on the reversed Brayton cycle. 2D aerodynamic compressor design and heat exchanger rating based on the P-NTU method have been successfully integrated in process chains together with cycle analysis. The number of assumptions about component performance during the phase of cycle design is lowered to the single parameter of turbine efficiency. This paper forms the basis for further investigations and the development of efficient structures for holistic optimization approaches. The latter will potentially impact the design of heat pumps and other complex systems in the long term as uncertainty in early design phases is reduced and detailed information on engine compactness and component costs can be considered.

The two introduced optimization approaches indicate that decoupling the design of heat exchangers (NHX) and thereby splitting the design vector increases robustness of convergence. Also, it can be stated that nested optimization loops work well with surrogate assisted global optimizations, if the problem is formulated in a way that unfeasible design requirements are traceable. Multi-objective optimizations for the trade-off between cycle performance and engine compactness have been successfully performed. The functionality of NHX is additionally underlined by the analysis of resulting component performance as well as by demonstrating the reproducibility of the results. It can be concluded, that the integration of complex component design is feasible for HTHP but it has to be noted that computational effort and stability are strongly dependent on the architecture of the optimization. The priorities for future research have been identified and are directly derived from this work. Generic approaches for component integration with intermediate response surfaces will be investigated.

REFERENCES

[1] Rehfeldt, Matthias, Fleiter, Tobias and Toro, Felipe. "A bottom-up estimation of the heating and cooling demand in European industry." *Energy Efficiency* Vol. 11 No. 5 (2018): pp. 1057–1082. DOI 10.1007/s12053-017-9571-y.

[2] Robert de Boer, Andrew Marina, Benjamin Zühlsdorf and Cordin Arpagaus. "Strengthening Industrial Heat Pump Innovation: Decarbonizing Industrial Heat." (2020).

[3] Arpagaus, Cordin, Bless, Frédéric, Uhlmann, Michael, Schiffmann, Jürg and Bertsch, Stefan S. "High temperature heat pumps: Market overview, state of the art, research status, refrigerants, and application potentials." *Energy* Vol. 152 (2018): pp. 985–1010. DOI 10.1016/j.energy.2018.03.166.

[4] Marina, A., Spoelstra, S., Zondag, H. A. and Wemmers, A. K. "An estimation of the European industrial heat pump market potential." *Renewable and Sustainable Energy Reviews* Vol. 139 (2021): p. 110545. DOI 10.1016/j.rser.2020.110545.

[5] Johannes Oehler, Jens Gollasch, A. Phong Tran and Eberhard Nicke. "Part Load Capability of a High Temperature Heat Pump with Reversed Brayton Cycle." *13th IEA Heat Pump Conference*. 2021.

[6] Gollasch, Jens Oliver, Agelidou, Eleni, Henke, Martin and Stathopoulos, Panagiotis (eds.). *Conceptual Study of Thermally Coupled Micro Gas Turbines and High Temperature Heat Pumps for Trigeneration*. DOI 10.1115/GT2022-81959.

[7] Lampe, Matthias, de Servi, Carlo, Schilling, Johannes, Bardow, André and Colonna, Piero. "Toward the Integrated Design of Organic Rankine Cycle Power Plants: A Method for the Simultaneous Optimization of Working Fluid, Thermodynamic Cycle, and Turbine." *Journal of Engineering for Gas Turbines and Power* Vol. 141 No. 11 (2019). DOI 10.1115/1.4044380.

[8] Persky, Rodney, Sauret, Emilie and Ma, Lin. "Optimisation Methods for Coupled Thermodynamic and 1D Design of Radial-Inflow Turbines." 2014. American Society of Mechanical Engineers. DOI 10.1115/FEDSM2014-21665.

[9] Schuster, Sebastian, Markides, Christos N. and White, Alexander J. "Design and off-design optimisation of an organic Rankine cycle (ORC) system with an integrated radial turbine model." *Applied Thermal Engineering* Vol. 174 (2020): p. 115192. DOI 10.1016/j.applthermaleng.2020.115192.

[10] Bahamonde, Sebastian, Pini, Matteo, de Servi, Carlo, Rubino, Antonio and Colonna, Piero. "Method for the Preliminary Fluid Dynamic Design of High-Temperature Mini-Organic Rankine Cycle Turbines." *Journal of Engineering for Gas Turbines and Power* Vol. 139 No. 8 (2017). DOI 10.1115/1.4035841.

[11] Tacconi, J., Visser, W. P. J. and Verstraete, D. "Multi-objective optimisation of semi-closed cycle engines for high-altitude UAV propulsion." *The Aeronautical Journal* Vol. 123 No. 1270 (2019): pp. 1938–1958. DOI 10.1017/aer.2019.62.

[12] Jens Schmeink, Markus Schnoes. "Automated Component Preliminary Design and Evaluation in the Overall Engine Using Fully Coupled Approaches." .

[13] Hendler, Marco, Lockan, Michael, Bestle, Dieter and Flassig, Peter. "Component-Specific Preliminary Engine Design Taking into Account Holistic Design Aspects." *International Journal of Turbomachinery, Propulsion and Power* Vol. 3 No. 2 (2018): p. 12. DOI 10.3390/ijtpp3020012.

[14] Meroni, Andrea, Zühlsdorf, Benjamin, Elmegaard, Brian and Haglind, Fredrik. "Design of centrifugal compressors for heat pump systems." *Applied Energy* Vol. 232 (2018): pp. 139–156. DOI 10.1016/j.apenergy.2018.09.210.

[15] Andrea Giuffre, Federica Ascione, Carlo De Servi and Matteo Pini. "DATA-DRIVEN MODELING OF HIGH-SPEED CENTRIFUGAL COMPRESSORS FOR AIRCRAFT ENVIRONMENTAL CONTROL SYSTEM: GPPS-TC-2022-0091." *Proceedings of Global Power and Propulsion Society*. 2022.

[16] Reitenbach, Stanislaus, Krumme, Alexander, Behrendt, Thomas, Schnös, Markus, Schmidt, Thomas, Hönig, Sandrine, Mischke, Robert and Mörland, Erwin. "Design and Application of a Multidisciplinary Predesign Process for Novel Engine Concepts." *Journal of Engineering for Gas Turbines and Power* Vol. 141 No. 1 (2019). DOI 10.1115/1.4040750.

[17] Richard-Gregor Becker and Florian Wolters and Mobin Nauroz and Tom Otten. "DEVELOPMENT OF A GAS TURBINE PERFORMANCE CODE AND ITS APPLICATION TO PRELIMINARY ENGINE DESIGN." *DLRK*. 2011.

[18] Schnoes, Markus, Voß, Christian and Nicke, Eberhard. "Design optimization of a multi-stage axial compressor using throughflow and a database of optimal airfoils." *Journal of the Global Power and Propulsion Society* Vol. 2 (2018): p. W5N91I. DOI 10.22261/JGPPS.W5N91I.

[19] Markus Schnoes, Eberhard Nicke. "Exploring a Database of Optimal Airfoils for Axial Compressor Design: ISABE-2017-21493." .

[20] Markus Schnoes and Eberhard Nicke. "Automated Calibration of Compressor Loss and Deviation Correlations." *Proceedings of ASME Turbo Expo 2015: Turbine Technical Conference and Exposition* (2015).

[21] C.C. Koch. "Stalling Pressure Rise Capability of Axial Flow Compressor Stages." *ASME Journal of Engineering for Power* Vol. Vol. 103/645 (1981).

[22] Springer-Verlag GmbH. *VDI-Wärmeatlas*. Springer Berlin Heidelberg, Berlin, Heidelberg (2013). DOI 10.1007/978-3-642-19981-3.

[23] Rainer Storn and Kenneth Price. "Differential Evolution: A Simple and Efficient Heuristic for global Optimization over Continuous Spaces." *Journal of Global Optimization* Vol. 11 (1996): pp. 341–359.

[24] Voß, Christian und Aulich, Marcel und Raitor, Till. "Metamodel Assisted Aeromechanical Optimization of a Transonic Centrifugal Compressor." *ISROMAC 15*. 2014.